Stem Cell Research 81 (2024) 103594

Contents lists available at ScienceDirect

Stem Cell Research

journal homepage: www.elsevier.com/locate/scr

Lab Resource: Genetically-Modified Multiple Cell Lines

Generation and characterization of two isogenic induced pluripotent stem cell lines from a young female with microcephaly carrying a compound heterozygous mutation in *BUB1* gene

Anita Ferreira [a,b,1], Sofia M. Calado [a,1,2], Xavier Jorge [a,b], Job de Lange [c], Sara Carvalhal [a,b,*]

[a] Algarve Biomedical Center, Research Institute (ABC-Ri), University of Algarve Campus Gambelas, Faro 8005-139, Portugal
[b] Algarve Biomedical Center (ABC), University of Algarve Campus Gambelas, Faro 8005-139, Portugal
[c] Cancer Center Amsterdam, Amsterdam University Medical Centers, Oncogenetics Section, De Boelelaan 1118, 1081 HV Amsterdam, Netherlands (the)

ARTICLE INFO

Keywords:
BUB1
Neurodevelopmental disorders
iPSC
Autosomal Recessive Primary Microcephaly (MCPH)
Autosomal Recessive Primary Microcephaly 30 (MCPH 30)
Cohesinopathy
Mosaic variegated aneuploidy (MVA) syndrome

ABSTRACT

Mutations in the Budding uninhibited by benzimidazoles (*BUB1*) gene were recently associated with neurodevelopmental disorders (Carvalhal et al., 2022). Here, we describe the generation and characterization of two induced pluripotent stem cells (iPSC) clones from a young female with microcephaly. The patient carried two variants in the *BUB*fibroblast gene (OMIM # 602452), one (c.[2197dupG]; p.[D732fs*11]) paternally inherited and one (c.[2625+1G>A]; p.[V822_L875del] maternally inherited. The generated clones exhibit a normal karyotype (UALGi003-A) and trisomy 8 (UALGi003-B), express pluripotency markers, and differentiate into trilineage cells in vitro. These cell lines can be used to study neurodevelopment and the processes of chromosome segregation.

1. Resource Table

Unique stem cell line identifier	UALGi003-A UALGi003-B
Alternative name(s) of stem cell line	BUB1P2-iPSC Cl1 (UALGi003-A) BUB1P2-iPSC Cl2 (UALGi003-B)
Institution	Universidade do Algarve, Faro, Portugal Algarve Biomedical Center Research Institute (ABC-Ri), Faro, Portugal
Contact information of distributor	sibandarra@ualg.pt
Type of cell line	iPSC
Origin	Human skin biopsy
Additional origin info required for human ESC or iPSC	Age: 16 Sex: Female Ethnicity: Turkish descent with Bulgarian ancestry
Cell source	Primary skin fibroblasts cells
Clonality	Clonal
Method of reprogramming	Non-integrating method (CyTo-Tune – iPS2.0 Sendai Reprogramming Kit) containing three vectors: polycistronic KOS (Klf4–Oct3/4–Sox2), cMyc, and Klf4.
Genetic Modification	No for BUB1P2-iPSC Cl1. Yes, for BUB1P2-iPSC Cl2.
Type of Modification	Spontaneous chromosomal abnormality (trisomy 8) on BUB1P2-iPSC Cl2.
Associated disease	Autosomal Recessive Primary Microcephaly 30 (MCPH 30) CohesinopathyMosaic variegated aneuploidy (MVA) syndrome
Gene/locus	BUB1 gene chr2:111,395,275–111,435,691 (GRCh37/hg19 by Ensembl) The paternal allele contains a c.[2197dupG]; p.[D732fs*11], and the maternal allele contains c.[2625+1G>A]; p.[V822_L875del].
Date archived/stock date	2024 August
Cell line repository/bank	https://hpscreg.eu/user/cellline/edit/UALGi003-A https://hpscreg.eu/user/cellline/edit/UALGi003-B
Ethical approval	Ethical approval by the AD-ABC Health Ethics Committee for the project "Quantitative Cohesin

(continued on next column)
(continued)
(continued on next page)

* Corresponding author.
E-mail address: sibandarra@ualg.pt (S. Carvalhal).
[1] Co-first authors.
[2] Current Address: University of Açores, Department of Sciences and Technology, 9500-321, Ponta Delgada, Portugal.

https://doi.org/10.1016/j.scr.2024.103594
Received 15 August 2024; Received in revised form 27 September 2024; Accepted 19 October 2024
Available online 23 October 2024

(*continued*)

	and Mitotic Fidelity in the Context of Cohesinopathies" (PI: S.Carvalhal).

2. Resource utility

Generated iPSC cell lines arise from one of the first two patients with biallelic germline *BUB1* mutations. This neurodevelopmental disorder shares characteristics with MCPH, MVA, and cohesinopathies (Carvalhal et al. 2022). This resource aids in studying these syndromes and their clinical features, as well as understanding BUB1′s cellular functions.

3. Resource details

Primary microcephaly is a common condition of many neurodevelopmental disorders. It is characterized by a head circumference at birth with more than 2 fold standard deviations below the mean for a specific age and sex (Jayaraman et al., 2018; Woods 2004). Mutations in mitotic genes, like *BUB1*, are frequently implicated in the development of microcephaly (Degrassi et al., 2019; Dolk 1991; Jayaraman et al., 2018). In concordance, two individuals with biallelic mutations in the *BUB1* gene with microcephaly have been described. Together with microcephaly, the described female patient displays slight growth retardation, Axenfeld Rieger anomaly at both eyes, Acanthosis nigricans neck, two cafe au lait spots at skin, mild intellectual disability and small congenital heart anomaly (atrial septal defect) (Carvalhal et al. 2022). SV40-transformed fibroblast cells express reduced levels of BUB1 protein with impaired kinase activity and display multiple mitotic defects including aneuploidy and defective sister chromatid cohesion (Carvalhal et al. 2022). However, the molecular mechanism underlying primary microcephaly and *BUB1* mutations in microcephaly are not fully understood. Generation of iPSCs carrying microcephaly-causing mutations has emerged as one critical approach in modelling neurodevelopmental disorders. In this study, we generated two iPSC clones carrying *BUB1* variants c.[2625+1G>A] mat;[c.2197dupG] pat (Carvalhal et al. 2022) which are free of mycoplasma (Fig. S1A). Table 1 contains a summary of the characterization carried-out on these cell lines. Sendai virus-free iPSCs clones (Fig. S1B) form colonies with a standard stem-like morphology visible by phase contrast (Fig. 1A). They are positive for Alkaline Phosphatase (AP) activity (Fig. 1B) and have positive immunofluorescence staining for the expression of pluripotent markers NANOG, OCT4, SOX2, and SSEA-4 (Fig. 1C). Moreover, key pluripotency SSEA-4 and TRA1-60 were detected by flow cytometry in the cell surface of both clones where P2 (orange dots) presents the respective percentages of positive cells: 100; 99.4; 99.7 and 97.3 %. (Fig. 1D). Clones were attested spontaneous *in vitro* differentiation ability after embryoid body (EB) formation. These showed positive staining for all three germ layers: ectoderm (TUJ1), mesoderm (α-SMA) and endoderm (AFP) (Fig. 1E). BUB1P2-iPSC Cl1 displays a normal diploid karyotype (46, XX) and BUB1P2-iPSC Cl2, a trisomy 8 (47, XX, +8) (Fig. 1F), in accordance with the described potential genomic instability of P2 primary cells (Carvalhal et al. 2022). Genetic signature identity and heterozygous carriership of the variant of iPSCs and patient fibroblasts were confirmed by DNA fingerprinting of 16 distinct loci and Sanger sequencing (Fig. 1G).

4. Materials and methods

4.1. Reprogramming of fibroblasts

P2 primary fibroblasts were cultivated as in (Carvalhal et al. 2022). Reprogramming was based on feeder-dependent CytoTune™-iPS 2.0 Sendai Reprogramming Kit user guide (Invitrogen™). Briefly, 175,000 fibroblasts were plated two days before transduction. Cells were transduced with MOI of 5–5–3 KOS, c-Myc, Klf4, respectively. Upon first passage, cells were seeded on a feeder layer of Mitomycin C-inactivated fibroblasts (ATCC-SCRC-1041). Cell colonies were manually picked and expanded in feeder cell plates. iPSCs were maintained at 37 °C in 5 % CO_2 in feeder-free mTeSR1 medium (STEMCell technologies) with 0,25 % P/S on 1 % Geltrex™(Gibco)-coated plates. Medium was refreshed daily, and cells regularly tested for mycoplasma (passage 3 onwards every other month; Table 2).

4.2. In vitro differentiation assay

For static suspension culture, 10,000 single cells were resuspended in 0,4% polyvinyl alcohol (Sigma) mTeSR medium with 10 μM Y-27632 in low-attachment plates. After 48 h, embryonic bodies (EB) were covered with complete DMEM. EBs kept in Geltrex-coated coverslips at 37 °C in 5 % CO_2, with medium changes every other day to fresh medium without Y-27632.

4.3. Immunofluorescence

Cells (passage 13–21) stained with NANOG, SOX2, OCT4 and α-SMA were fixed for 10 min in 4 % PFA-PBS. SEEA4 was fixed similarly followed by 10 min of permeabilization with 0.5 % EH9-PBS (ITW reagents, TX-100 replacement). TUJ1 was fixed for 10 min in 4 % PFA-PBS then permeabilized 15 min in 0.5 % EH9- PBS. AFP was fixed instead for 5 min and permeabilized 5 min in 0.1 % EH9-PBS. After fixation and/or permeabilization, coverslips were incubated for 5 min in 0.1 % EH9-TBS, and twice in 0.1 % EH9-PBS (PBS-Wash). Blocking and antibody dilution buffer was done as described in (S. Carvalhal et al. 2015)where primary antibodies (Table 2) were incubated at 4 °C for 16 h and secondary antibodies at room temperature (25 °C), 1 h with 5 μg/mL Hoechst 34,580 (ThermoFisher). Excess antibodies were removed by three washes with PBS-Wash for 5 min. Coverslips were mounted in Vectashield (Vector Laboratories). Fixed cells were acquired on Axioimager Z2 flourescence microscope (Zeiss) with 5-40x APO objective lens (Olympus), CoolSNAP HQ camera (Photometrics), and standard filter sets.

4.4. Flow cytometry

Pre-washed dissociated iPSCs (passage 10–11) were incubated on ice for 30–40 min with conjugated-antibodies (Table2) diluted in 1 % BSA PBS. Excess antibodies were removed by two washed with 1 % BSA PBS. Resuspended cells in PBS1x were analysed on the CytoFlex Flow Cytometer (Beckman Coulter) and processed using FlowJo™ Software. Unstained cells were used as control.

4.5. Alkaline phosphatase activity

Cells were stained using Alkaline Phosphatase Staining Kit II (Stemgent®) following manufacturer's instructions.

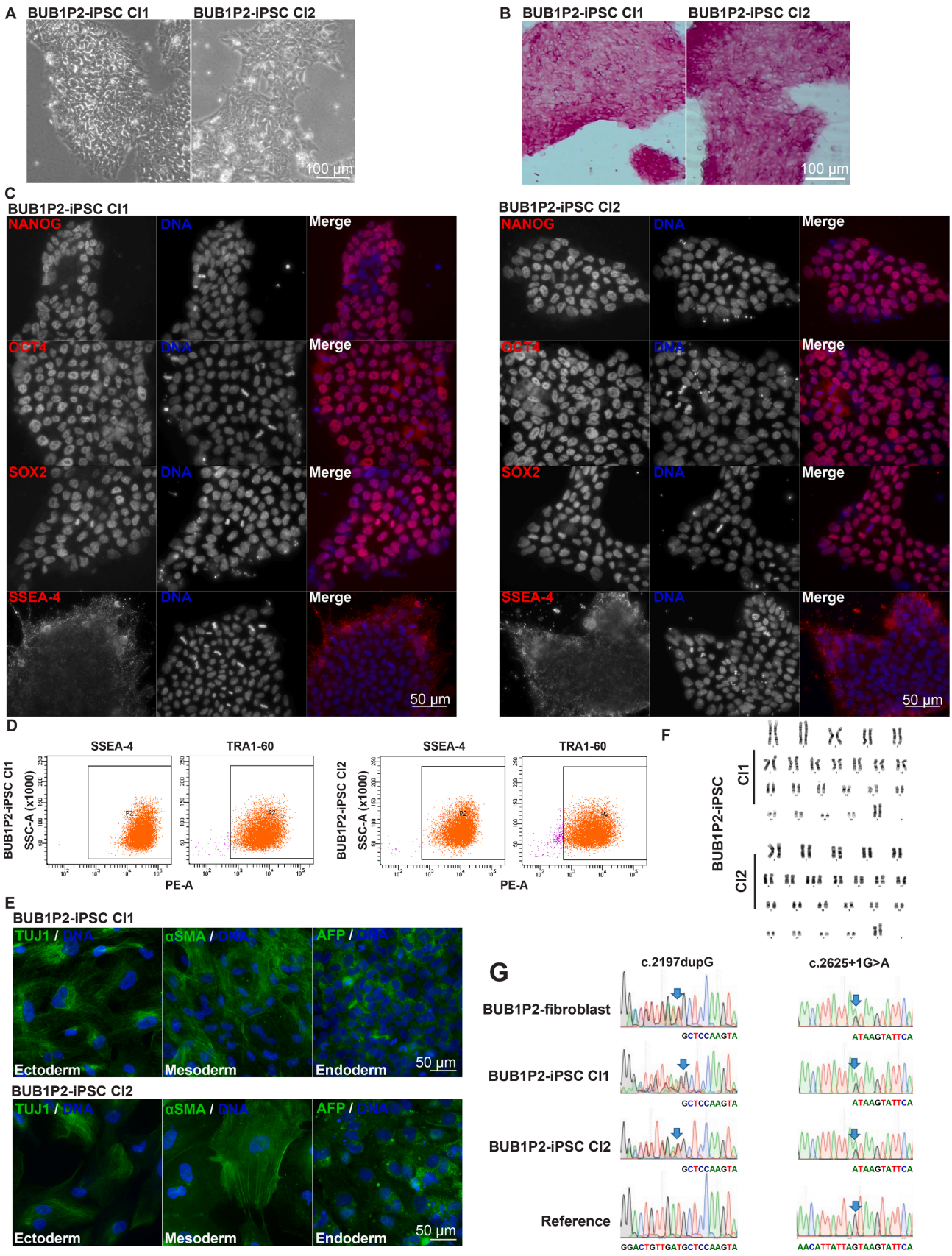

Fig. 1. Characterization of the BUB1P2-iPSC Cl1 (UALGi003-A) and BUB1P2-iPSC Cl2 (UALGi003-B) lines.

Table 1
Summary characterization and validation results obtained for both BUB1P2-iPSC clones.

Classification	Test	Result		Data
Morphology	Photography (phase-contrast image)	Typical iPSC morphology		Fig. 1A
Pluripotency status evidence	Qualitative analysis (immunofluorescence)	Positive staining of pluripotency markers: Alkaline Phosphatase, NANOG, OCT4, SOX2, SSEA-4		Fig. 1BFig. 1C
	Quantitative analysis (flow cytometry)	BUB1P2-iPSC Cl1 99,4% TRA1-60 100 % SSEA-4	BUB1P2-iPSC Cl2 97,3% TRA1-60 99,7% SSEA-4	Fig. 1D
Karyotype	Karyotype (G-banding) and resolution	BUB1P2-iPSC Cl1 46 XX [30], Resolution 400–500	BUB1P2-iPSC Cl2 47, XX, +8 [26], Resolution 400–500	Fig. 1F
Parental and modified cell line genetic identity evidence	STR analysis	All 16 loci matched		N.A.
Mutation analysis	Sequencing	Heterozygous carriership of the variant by DNA sequencing, matched		Fig. 1 G
Microbiology and virology	Mycoplasma	Mycoplasma testing by PCR: negative		Fig. S1A
Differentiation potential	Spontaneous differentiation of embryoid body	Ectoderm: TUJ1 (TUBB3) Endoderm: AFP Mesoderm: α-SMA		Fig. 1E

Table 2
Reagents details.

	Antibodies used for immunocytochemistry/flow-cytometry			
	Antibody	Dilution	Company Cat #	RRID
Pluripotency Markers (immunofluorescence and flow cytometry)	Rabbit anti-NANOG	1:400	Cell Signaling Technology Cat# 4903	AB_10559205
	Rabbit anti-OCT4	1:400	Cell Signaling Technology Cat# 2840	AB_2167691
	Mouse anti-SSEA-4	1:100	BD Biosciences Cat# 560073	AB_1645601
	Rabbit anti-SOX2	1:400	Cell Signaling Technology Cat# 3579	AB_2195767
	PE anti-human TRA-1-60-R	1:50	BioLegend Cat#330610	AB_2119065
	PE anti-human SSEA-4	1:40	BioLegend Cat#330406	AB_1089206
Differentiation Markers	Mouse anti-AFP	1:100	Millipore Cat# SCR030	AB_597591
	Mouse anti-ASM	1:500	Sigma-Aldrich Cat#A5228	AB_262054
	Mouse anti-TUBB3 (TUJ-1)	1:500	BioLegend Cat#801201	AB_2313773
Secondary antibodies	Donkey anti-Mouse 488	1:500	Molecular Probes Cat# A-21202	AB_141607
	Goat anti-Mouse 568	1:500	Molecular Probes Cat# A-A11031	AB_144696
	Donkey anti-Rabbit 488	1:500	Molecular Probes Cat# A-21206	AB_2535792
	Goat anti-Rabbit 568	1:500	Molecular Probes Cat# A-11011	AB_143157
	Primers			
	Target	**Size of band**	**Forward/Reverse primer (5′-3′)**	
Mycoplasma (PCR)	M. arginine	500 bp	Forward primers:	
	M. boris		CGC CTG AGT AGT ACG TTC GC	
	M. fermentans		CGC CTG AGT AGT ACG TAC GC	
	M. hominis		TGC CTG AGT AGT ACA TTC GC	
	M. hyorhinis		CGC CTG GGT AGT ACA TTC GC	
	M. orale		CGC CTG AGT AGT ATG CTC GCTGC CTG GGT AGT ACA TTC GC	
			Reverse primers:	
			GCG GTG TGT ACA AGA CCC GA	
			GCG GTG TGT ACA AAA CCC GA	
			GCG GTG TGT ACA AAC CCC GA	

4.6. RT-PCR for detection of virus

Complementary DNA (cDNA) from iPSC (passage 13–14) was obtained using NZY Viral RNA Isolated kit (NZYTech) and cDNA synthesis kit (NZYTech). Real-time PCR was performed at QuantStudio™ 1 System using TaqMan® (ThermoFisher) guidelines for specific probes: SeV (Mr04269880_mr); KOS (Mr04421257_mr); Klf4 (Mr04421256_mr) and cMyc (Mr04269876_mr).

4.7. Genomic analysis

Genomic integrity of colcemid-arrested iPSCs was assessed by karyotyping (passage 5;20) at GenoMed; fingerprinting by STABVida using PowerPlex16 loci™; mutations analysis as in Carvalhal et al. 2022.

Credit authorship contribution statement

Anita Ferreira: Writing – original draft, Methodology, Investigation, Formal analysis, Data curation. **Sofia M. Calado:** Writing – review & editing, Supervision, Methodology, Investigation, Formal analysis. **Xavier Jorge:** Writing – review & editing, Visualization, Investigation, Formal analysis. **Job de Lange:** Writing – review & editing, Investigation, Funding acquisition, Formal analysis. **Sara Carvalhal:** Writing – review & editing, Writing – original draft, Supervision, Project administration, Investigation, Funding acquisition, Data curation, Conceptualization.

Declaration of competing interest

The authors declare that they have no known competing financial interests or personal relationships that could have appeared to influence the work reported in this paper.

Acknowledgments

We thank the technical support of ABC-Ri Imaging Facility and F. Esteves, R. Koppenol, A. Agostinho and I. Milagre for insightful discussions. This work was supported by Fundação para a Ciência e Tecnologia (FCT): CEECIND/03721/2018/CP1540/CT0003, (DOI 10.54499/CEECIND/03721/2018/CP1540/CT0003); 2020.01532.CEECIND; 2022.01028.PTDC (DOI 10.54499/2022.01028.PTDC) and ABC-Ri/ABC internal funding.

Appendix A. Supplementary data

Supplementary data to this article can be found online at https://doi.org/10.1016/j.scr.2024.103594.

References

Carvalhal, S., Ribeiro, S.A., Arocena, M., Kasciukovic, T., Temme, A., Koehler, K., Huebner, A., Griffis, e E.R., 2015. The nucleoporin ALADIN regulates Aurora A localization to ensure robust mitotic spindle formation. Mol. Biol. Cell 26 (19). https://doi.org/10.1091/mbc.E15-02-0113.

Carvalhal, S., Bader, I., Rooimans, M.A., Oostra, A.B., Balk, J.A., Feichtinger, R.G., Beichler, C., et al., 2022. Biallelic *BUB1* mutations cause microcephaly, developmental delay, and variable effects on cohesion and chromosome segregation. Sci. Adv. 8 (3), eabk0114. https://doi.org/10.1126/sciadv.abk0114.

Degrassi, F., Damizia, M., e Patrizia Lavia, 2019. The Mitotic apparatus and kinetochores in microcephaly and neurodevelopmental diseases. Cells 9 (1), 49. https://doi.org/10.3390/cells9010049.

Dolk, H., 1991. The predictive value of microcephaly during the first year of life for mental retardation at seven years. Dev. Med. Child Neurol. 33 (11), 974–983. https://doi.org/10.1111/j.1469-8749.1991.tb14813.x.

Jayaraman, D., Bae, B.-I., Walsh, e C.A., 2018. The genetics of primary microcephaly. Annu. Rev. Genomics Hum. Genet. 19 (1), 177–200. https://doi.org/10.1146/annurev-genom-083117-021441.

Woods, C.G., 2004. Human microcephaly. Curr. Opin. Neurobiol. 14 (1), 112–117. https://doi.org/10.1016/j.conb.2004.01.003.